

The roles of metastasis-related proteins in the development of giant cell tumor of bone, osteosarcoma and Ewing's sarcoma

Bo Dou^{a,b,1}, Tianrui Chen^{c,1}, Qiubo Chu^b, Guirong Zhang^{b,*} and Zhaoli Meng^{a,*}

^aDepartment of Translational Medicine, First Hospital, Jilin University, Changchun, Jilin 130061, China

^bSchool of Life Sciences, Jilin University, Changchun, Jilin 130012, China

^cDepartment of Bone Tumor Surgery, Changzheng Hospital, Second Military Medical University, Shanghai 200003, China

Abstract.

BACKGROUND: Giant cell tumor of bone (GC), osteosarcoma (OS) and Ewing's sarcoma (ES) are three different types of bone cancer with common and specific pathology features.

OBJECTIVE: The purpose of the study was to examine the relationship and differences of the three bone tumors using clinical samples.

METHODS: Through screening the profiles of clinical samples from GC, OS and ES patients using a human oncology array, we found 26, 25 and 15 tumorigenesis factors significantly increased in GS, OS and ES tissues compared to normal individuals. eNOS, endostatin, HIF-1 α , IL-6, CCL2/MCP-1, CCL8/MCP-2, CCL7/MCP-3, Tie and VEGF directly or indirectly involve in the metastasis. Therefore, expression levels of the 6 factors were further determined by Western blot.

RESULTS: The results showed levels of MCP1, MCP2, MCP3 or IL-6 in the GS, OS and ES significantly increased, and the expression levels of angiogenesis and anti-angiogenesis factors containing eNOS, endostatin, HIF-1 α , Tie or VEGF were enhanced.

CONCLUSIONS: Our results suggest that eNOS, endostatin, HIF-1 α , IL-6, CCL2/MCP-1, CCL8/MCP-2, CCL7/MCP-3, Tie and VEGF may play important roles in tumorigenesis, reveal the expression differences of tumor-associated cytokines and angiogenesis related factors, and provide clinical evidence for studying the mechanisms on the metastasis in GC, OS and ES.

Keywords: Giant cell tumor of bone, osteosarcoma, Ewing's sarcoma, metastasis

1. Introduction

Giant cell tumor (GC) of bone, Osteosarcoma (OS) and Ewing Sarcoma (ES) are three different types of cancers that occur in bone. Majority of high-risk group suffering GC, OS and ES aged below 50 years old [1]. Especially, as the most common primary bone tumors, OS and ES usually occur in children, adolescents and young adults, and the 5-year overall survival rates have not been improved for patients with localized forms [2]. However, it is still difficult to distinguish OS from ES just by

¹Bo Dou and Tianrui Chen contributed equally to this work.

*Corresponding authors: Guirong Zhang, School of Life Sciences, Jilin University, Changchun, Jilin 130012, China. E-mail: zgr@jlu.edu.cn. Zhaoli Meng, Department of Translational Medicine, First Hospital, Jilin University, Changchun, Jilin 130061, China. Tel.: +86 431 8878 3044; E-mail: mengzl@jlu.edu.cn.

imaging examination methods. GC of bone usually occurs in patients with mature bone, and the patient mainly distributed in the 20 to 50-year age population. Therefore, there is an urgent need to identify the relationship between them.

GC is classified as an intermediate, rarely metastasizing tumor, and characterized by local destruction in bone that leads to significant osteolysis that accounting for approximately 6% of all primary bone tumors [3]. The giant cells are osteoclast-like cells that occasionally presented a cellular structural similarity, and expressed many characteristic factors of osteoclasts [4]. The neoplastic cells recruit reactive cells to the tumor stroma from bone marrow-derived monocytic cells and release specific cytokines to the tumor stroma. Additionally, numerous members of matrix metalloproteinase (MMP) family were identified in GC, which were expressed by giant cells or stromal cells [5], but there is little actual evidence mentioning any specific roles in tumor. OS is one of the most often suffering cancers in dogs, and an altered pro- and anti-inflammatory immunologic profile was determined in OS dogs, and have a high expression of insulin growth factor receptor type 2 [6]. Data show that cancer-associated fibroblasts alter the expression of pro-angiogenic and migratory factors in OS cell lines [7]. IL-6 involved in the proliferation of OS cells, and TGF β signal displayed an IL-6-dependence which could activate mesenchymal n-catenin, then promoted an inhibition of OS [8]. However, the current models used to study OS mainly focus on mouse and canine models. Research on OS using clinical samples might provide new insights for understanding the mechanisms of OS. ES predominantly afflict young patients with a high metastatic malignancy [9]. The tumorigenesis of ES sarcoma was proved to associate with vascular endothelial growth factor (VEGF). On the aspect of angiogenesis, ES tumor tissues express hypoxia-inducible factors (HIFs) in hypoxic center of tumor which are in response to lower oxygen levels. HIFs bind to the promoter region of VEGF, up-regulate the expression of VEGF in ES tumor cells and endothelial cells [10]. Through regulating the levels of VEGF, cellular and viral oncogenes not only regulate the growth of ES tumor cells, but also promote ES cancer progression. Above all, GC, OS and ES have their own pathogenic characteristics and similar features. However, up to date, little study has been performed to identify the cancer-associated cytokines among them. Investigating specific molecular factors might serve as a promoter for understanding the pathogenic mechanisms of the three bone tumors.

The aim of the present study was to investigate the cancer-associated factors in GC, ES and OS tissues. We could try to find out those factors which are widely associated with different types of bone cancer, and which may just correlated with specific type of bone cancer. Our study will provide new insight for the mechanism research of GC, ES and OS.

2. Materials and methods

2.1. Clinical samples information

A total of 28 bone tumor patients diagnosed with GC, OS or ES at Changzheng Hospital (Shanghai, China) from Dec. 2014 to Mar. 2016 were enrolled in the study. The number of GC, OS and ES samples is 14, 8 and 6, respectively. The patients included 16 males and 9 females, with an average age of 37.2 ± 15.9 years (range, 15–73 years). The research protocol was approved by the Ethics Committee of the Second Military Medical University, and written informed consent was obtained from all participants.

2.2. Proteome profiling analysis

Forty cancer-associated cytokines in clinical samples were detected by a human XL oncology array

kit (ARY026, R&D Systems, Millipore, USA). According to the instruction, clinical tumor tissues were preprocessed. The membrane was blocked with BSA for 1 h and then incubated with tissue protein mixed with a biotinylated detection antibody. Streptavidin-HRP and chemiluminescence were used to detect the primary antibodies. The binding to membranes were finally visualized and quantified with by ImageJ software version 1.51 (National Institutes of Health, Bethesda, MD, USA).

2.3. Western blotting analysis

Total protein extracted from clinical samples were homogenized with RIPA buffer (Sigma-Aldrich, USA) containing 1% protease inhibitor cocktail (Sigma-Aldrich, USA) and 0.5% phenylmethanesulfonyl fluoride (PMSF) (Sigma-Aldrich, USA). The protein concentration was detected by BCA protein assay kit (Merck Millipore, Germany). The protein lysate were boiled at 95°C for 6 minutes with loading buffer (Solarbio, China), separated by sodium dodecyl-sulfate polyacrylamide gel electrophoresis (SDS-PAGE) (PowerPac™ Basic300V Power Supply, bio-rad, CA, USA), electrophoretically transferred onto nitrocellulosemembranes (0.45 μm, Bio Basic Inc., Canada). After blocking in the 5% bovine serum albumin (BSA) (sigma, USA) solubilized with tris buffered saline (TBS), the membranes were incubated at 4°C for over 8 h, with primary antibodies against β-actin (sc-47778, Santa Cruz Biotechnology, USA), endostatin (ab64569, Abcam, Cambridge, MA, USA), endothelialnitric oxide synthase (eNOS) (ab76198, Abcam, Cambridge, MA, USA), hypoxia-inducible factor 1α (HIF-1α) (MAB5382, Merck Millipore, Germany), Interleukin 6 (IL-6) (ab214429, Abcam, Cambridge, MA, USA), monocyte chemoattractant protein 1 (MCP-1) (ab21396, Abcam, Cambridge, MA, USA), monocyte chemoattractant protein 2 (MCP-2) (ab83803, Abcam, Cambridge, MA, USA), monocyte chemoattractant protein 3 (MCP-3) (ab130340, Abcam, Cambridge, MA, USA), Angiopoietin-1 receptor (TIE-2) (ab24859, Abcam, Cambridge, MA, USA), vascular endothelial growth factor (VEGF) (ABS82, Merck Millipore, Germany). Those above antibodies are diluted according to the instructions with BSA solubilized TBS. Then the membranes were incubated with corresponding secondary antibody, goat anti-rabbit IgG (E-AB-1034, Elabscience Biotechnology, Wuhan, China) or goat anti-mouse IgG (E-AB-1035, Elabscience Biotechnology, Wuhan, China). Finally the blotting were developed by gel imaging system (6200 Luminescent Imaging Workstation, Tanon, China) with ECL detection kits (WBKLS0500, Merck Millipore, Germany). Quantitativegran-scale analysis was processed by Image J software version 1.51 (National Institutes of Health, Bethesda, MD, USA).

2.4. Statistical analysis

All values are presented as means ± SD. A one-way analysis of variance was used to calculate statistical significance, followed by Dunn's test using SPSS 22.0 (IBM, Armonk, NY, USA). $P < 0.05$ indicates statistical significance.

3. Results

3.1. Analysis of the expression levels of bone cancer-related protein in clinical samples

To systematically determine the potential factors that are relevant to carcinogenesis of bone, proteome profiling analysis was used to detect cancer-related protein levels on OS, GC and ES tissues (Fig. 1A). Compared with the normal bone tissues, the enhanced factors in OS, GC and ES were summarized in

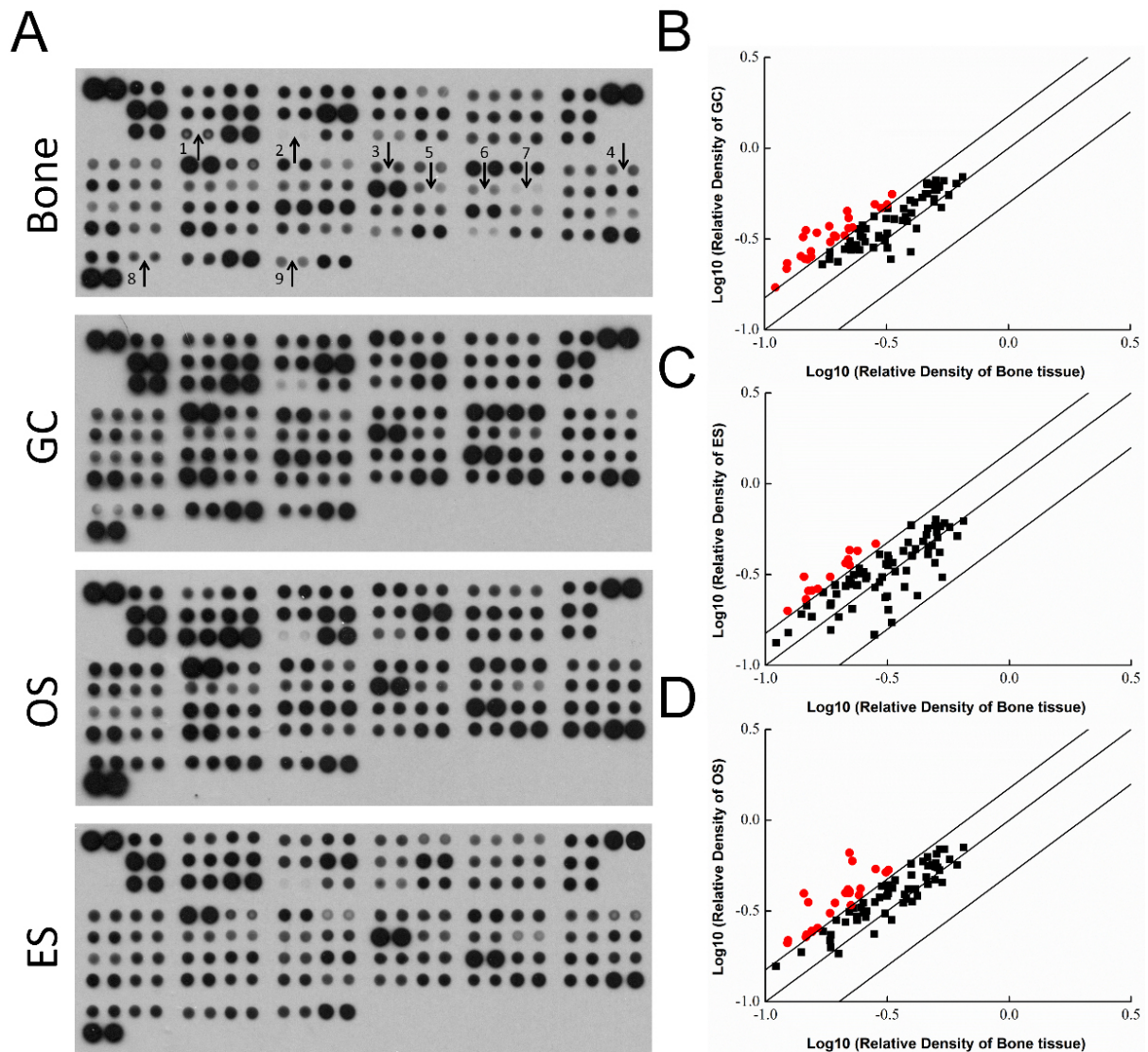


Fig. 1. The expression of oncology genes in GS, OS and ES clinical tissues. A. Graphical representation of genes expressions in GC, OS and ES. The arrows indicate the factors involved in the metastasis with a significant change $> 50\%$ (bone tumor group versus control group). B–D. Scatter diagram of 40 oncogenes. The relative density is determined as the ratio of the absolute value versus the reference spot value, the red spot indicated that the significantly changed factors. 26, 25 and 15 tumorigenesis factors significantly increased in GS (B), OS (C) and ES tissues (D).

Table 1. As shown in Fig. 1B, compared with normal bone tissues, 26 factors significantly increased in GC tissues, and they were BCL-x, endostatin, eNOS, ER α /NR3A1, GM-CSF, CG α / β (HCG), HGFR/c-Met, HIF-1 α , HNF-3 β , ICAM-1/CD54, IL-2R α , IL-6, Kallikrein 3/PSA, Kallikrein 5, Kallikrein 6, CCL2/MCP-1, CCL8/MCP-2, CCL7/MCP-3, Nectin-4, p27/Kip1, PDGF-AA, Serpin B5/Maspin, Snail, SPARC, Urokinase and VEGF. Twenty-five factors expression levels significantly increased in OS samples compared to that of the control, they were BCL-x, endostatin, eNOS, pCAM/TROP1, ErbB2, FoxC2, FoxO1/FKHR, GM-CSF, HGF R/c-Met, HIF-1 α , HNF-3 β , IL-2R α , IL-6, CCL2/MCP-1, CCL8/MCP-

Table 1
The quantitative outcome of proteome profiling analysis

Coordinate and target	Human bone cancer								
	Pixel density			Pixel density			Pixel density		
	Bone	GC	Fold	Bone	OS	Fold	Bone	ES	Fold
α -Fetoprotein	0.5315	0.4710	0.8861	0.5315	0.4532	0.8527	0.5315	0.3052	0.5742
Amphiregulin	0.2799	0.2833	1.0122	0.2799	0.2362	0.8438	0.2799	0.1470	0.5253
Angiopoietin-1	0.4206	0.3612	0.8588	0.4206	0.3826	0.9097	0.4206	0.2418	0.5749
Angiopoietin-like 4	0.2940	0.3199	1.0881	0.2940	0.3752	1.2764	0.2940	0.2867	0.9753
ENPP-2/Autotaxin	0.3787	0.4206	1.1105	0.3787	0.3667	0.9683	0.3787	0.3324	0.8778
Axl	0.3725	0.4648	1.2478	0.3725	0.3906	1.0487	0.3725	0.2698	0.7242
BCL-x	0.1549	0.2706	1.7477	0.1549	0.2456	1.5858	0.1549	0.1854	1.1970
CA125/MUC16	0.1853	0.2668	1.4401	0.1853	0.1989	1.0735	0.1853	0.1563	0.8433
E-Cadherin	0.1998	0.2369	1.1859	0.1998	0.1837	0.9196	0.1998	0.1842	0.9222
VE-Cadherin	0.4004	0.4407	1.1005	0.4004	0.3562	0.8895	0.4004	0.4023	1.0047
CapG	0.6496	0.6951	1.0700	0.6496	0.7081	1.0901	0.6496	0.6221	0.9577
Carbonic Anhydrase IX	0.3400	0.4066	1.1959	0.3400	0.4670	1.3737	0.3400	0.3287	0.9668
Cathepsin B	0.4652	0.6291	1.3522	0.4652	0.5599	1.2034	0.4652	0.4500	0.9674
Cathepsin D	0.3159	0.4098	1.2969	0.3159	0.3828	1.2116	0.3159	0.2396	0.7585
Cathepsin S	0.6129	0.6389	1.0423	0.6129	0.5664	0.9242	0.6129	0.5147	0.8398
CEACAM-5	0.3299	0.2445	0.7411	0.3299	0.2824	0.8559	0.3299	0.1717	0.5204
Decorin	0.4444	0.5346	1.2029	0.4444	0.5913	1.3305	0.4444	0.4810	1.0823
Dkk-1	0.3194	0.2831	0.8864	0.3194	0.3948	1.2361	0.3194	0.2019	0.6322
DLL1	0.3098	0.3190	1.0297	0.3098	0.3061	0.9882	0.3098	0.2360	0.7617
EGF R/ErbB1	0.4644	0.5608	1.2076	0.4644	0.4435	0.9552	0.4644	0.4071	0.8766
Endoglin/CD105	0.5034	0.6648	1.3207	0.5034	0.6510	1.2932	0.5034	0.5398	1.0723
Endostatin	0.2211	0.4132	1.8686	0.2211	0.6611	2.9901	0.2211	0.4305	1.9471
Enolase 2	0.5429	0.6614	1.2183	0.5429	0.6916	1.2738	0.5429	0.6056	1.1154
eNOS	0.0152	0.0485	3.1989	0.0152	0.0390	2.5731	0.0152	0.0167	1.1017
EpCAM/TROP1	0.2271	0.2748	1.2103	0.2271	0.5950	2.6202	0.2271	0.2043	0.8995
ER α /NR3A1	0.1106	0.1709	1.5458	0.1106	0.1569	1.4191	0.1106	0.1333	1.2051
ErbB2	0.2423	0.3591	1.4819	0.2423	0.3866	1.5955	0.2423	0.3409	1.4067
ErbB3/Her3	0.2214	0.2869	1.2959	0.2214	0.3128	1.4132	0.2214	0.2798	1.2638
ErbB4	0.2374	0.2831	1.1925	0.2374	0.2951	1.2428	0.2374	0.2766	1.1651
FGF basic	0.2939	0.3293	1.1205	0.2939	0.3750	1.2757	0.2939	0.4072	1.3855
FoxC2	0.2454	0.2758	1.1238	0.2454	0.4201	1.7116	0.2454	0.3193	1.3009
FoxO1/FKHR	0.2212	0.2819	1.2741	0.2212	0.4061	1.8355	0.2212	0.3569	1.6132
Galectin-3	0.5207	0.6192	1.1893	0.5207	0.6902	1.3255	0.5207	0.5839	1.1214
GM-CSF	0.2207	0.3628	1.6439	0.2207	0.3970	1.7990	0.2207	0.2968	1.3450
CG α/β (HCG)	0.3179	0.4892	1.5386	0.3179	0.4394	1.3821	0.3179	0.4020	1.2645
HGF R/c-Met	0.1238	0.2326	1.8787	0.1238	0.2180	1.7613	0.1238	0.1511	1.2209
HIF-1 α	0.2130	0.3309	1.5537	0.2130	0.3975	1.8665	0.2130	0.3650	1.7138
HNF-3 β	0.1931	0.3310	1.7147	0.1931	0.3502	1.8141	0.1931	0.2764	1.4316
HO-1/HMOX1	0.4575	0.5601	1.2242	0.4575	0.4856	1.0614	0.4575	0.5229	1.1429
ICAM-1/CD54	0.3331	0.5586	1.6771	0.3331	0.4221	1.2671	0.3331	0.3671	1.1020
IL-2 R α	0.1475	0.3530	2.3926	0.1475	0.2347	1.5908	0.1475	0.2134	1.4461
IL-6	0.1231	0.2172	1.7644	0.1231	0.2108	1.7120	0.1231	0.1995	1.6203
CXCL8/IL-8	0.3853	0.3955	1.0264	0.3853	0.4165	1.0809	0.3853	0.4737	1.2293
IL-18 BPa	0.2475	0.3282	1.3261	0.2475	0.3300	1.3334	0.2475	0.3256	1.3158
Kallikrein 3/PSA	0.1958	0.3248	1.6589	0.1958	0.2810	1.4352	0.1958	0.2466	1.2594
Kallikrein 5	0.1406	0.2541	1.8066	0.1406	0.1873	1.3318	0.1406	0.1915	1.3616
Kallikrein 6	0.1859	0.3047	1.6386	0.1859	0.2338	1.2572	0.1859	0.2189	1.1775
Leptin	0.2610	0.3607	1.3822	0.2610	0.3159	1.2104	0.2610	0.3096	1.1863
Lumican	0.4997	0.5868	1.1743	0.4997	0.5816	1.1638	0.4997	0.6347	1.2700
CCL2/MCP-1	0.1551	0.2527	1.6290	0.1551	0.2423	1.5620	0.1551	0.2584	1.6655
CCL8/MCP-2	0.1841	0.3724	2.0226	0.1841	0.3079	1.6723	0.1841	0.3072	1.6687

Table 1, continued

Coordinate and target	Human bone cancer								
	Pixel density			Pixel density			Pixel density		
	Bone	GC	Fold	Bone	OS	Fold	Bone	ES	Fold
CCL7/MCP-3	0.0838	0.2445	2.9168	0.0838	0.1640	1.9571	0.0838	0.1544	1.8417
M-CSF	0.2811	0.4209	1.4975	0.2811	0.3534	1.2573	0.2811	0.2680	0.9535
Mesothelin	0.3187	0.3405	1.0682	0.3187	0.4094	1.2846	0.3187	0.3544	1.1121
CCL3/MIP-1 α	0.1725	0.2294	1.3298	0.1725	0.2438	1.4134	0.1725	0.2516	1.4585
CCL20/MIP-3 α	0.2383	0.2796	1.1731	0.2383	0.2870	1.2040	0.2383	0.4270	1.7916
MMP-2	0.3197	0.4665	1.4589	0.3197	0.5317	1.6629	0.3197	0.3846	1.2027
MMP-3	0.3680	0.4005	1.0885	0.3680	0.3500	0.9511	0.3680	0.4258	1.1572
MMP-9	0.4959	0.5057	1.0197	0.4959	0.4692	0.9461	.4959	0.3664	0.7389
MSP/MST1	0.4966	0.5255	1.0582	0.4966	0.5536	1.1148	0.4966	0.5881	1.1843
MUC-1	0.2525	0.3246	1.2854	0.2525	0.3097	1.2264	0.2525	0.3265	1.2931
Nectin-4	0.2297	0.3655	1.5914	0.2297	0.3287	1.4312	0.2297	0.3139	1.3667
Osteopontin (OPN)	0.4624	0.6422	1.3887	0.4624	0.6254	1.3524	0.4624	0.5678	1.2278
p27/Kip1	0.2184	0.4515	2.0675	0.2184	0.4161	1.9055	0.2184	0.3832	1.7550
p53	0.2524	0.3758	1.4886	0.2524	0.3504	1.3881	0.2524	0.3261	1.2918
PDGF-AA	0.1638	0.3425	2.0908	0.1638	0.2551	1.5572	0.1638	0.2637	1.6102
CD31/PECAM-1	0.5083	0.5883	1.1573	0.5083	0.5495	1.0810	0.5083	0.5050	0.9934
Progesterone R/NR3C3	0.2136	0.2776	1.2997	0.2136	0.2748	1.2867	0.2136	0.2733	1.2798
Progranulin	0.4824	0.6325	1.3112	0.4824	0.5656	1.1725	0.4824	0.4572	0.9477
Prolactin	0.2379	0.2927	1.2301	0.2379	0.2806	1.1796	0.2379	0.2744	1.1532
Prostasin/Prss8	0.2586	0.3054	1.1810	0.2586	0.2928	1.1325	0.2586	0.3003	1.1615
E-Selectin/CD62E	0.1844	0.2442	1.3242	0.1844	0.2179	1.1819	0.1844	0.2137	1.1591
Serpin B5/Maspin	0.1465	0.2456	1.6762	0.1465	0.2275	1.5525	0.1465	0.2309	1.5753
Serpin E1/PAI-1	0.4135	0.5023	1.2148	0.4135	0.4162	1.0065	.4135	0.4362	1.0550
Snail	0.1439	0.3246	2.2561	0.1439	0.3954	2.7479	0.1439	0.3078	2.1391
SPARC	0.2836	0.4913	1.7323	0.2836	0.5386	1.8991	0.2836	0.4668	1.6460
Survivin	0.3121	0.3099	0.9931	0.3121	0.5164	1.6548	0.3121	0.3616	1.1587
Tenascin C	0.5702	0.5517	0.9674	0.5702	0.6083	1.0668	0.5702	0.5771	1.0120
Thrombospondin-1	0.3978	0.2685	0.6749	0.3978	0.4985	1.2532	0.3978	0.3991	1.0034
Tie-2	0.2242	0.3077	1.3721	0.2242	0.3408	1.5196	0.2242	0.2826	1.2603
Urokinase	0.3009	0.4679	1.5550	0.3009	0.4330	1.4390	0.3009	0.3064	1.0181
VCAM-1/CD106	0.5195	0.6079	1.1700	0.5195	0.5308	1.0216	0.5195	0.4191	0.8066
VEGF	0.1499	0.2448	1.6330	0.1499	0.3535	2.3582	0.1499	0.2572	1.7157
Vimentin	0.3964	0.5168	1.3037	0.3964	0.5758	1.4524	0.3964	0.5898	1.4878

2, CCL7/MCP-3, MMP-2, p27/Kip1, PDGF-AA, Serpin B5/Maspin, Snail, SPARC, Survivin, Tie-2 and VEGF (Fig. 1C). In ES samples, only 14 factors were significantly higher than the normal bone tissues, they were endostatin, FoxO1/FKHR, HIF-1 α , IL-6 CCL2/MCP-1, CCL8/MCP-2, CCL7/MCP-3, CCL20/MIP-3 α , p27/Kip1, PDGF-AA, Serpin B5/Maspin, Snail, SPARC and VEGF (Fig. 1D). Our data showed that CG α/β (HCG), ICAM-1/CD54, Kallikrein 3/PSA, Kallikrein 5 and Kallikrein 6 only increased in GC tissues, pCAM/TROP1, ErbB2, FoxC2 and HGF R/c-Met only increased in OS tissues, and CCL20/MIP-3 α only increased in ES samples, and FoxO1/FKHR expressed higher in both OS and ES samples. In the three bone tumor tissues, 12 factors including endostatin, HIF-1 α , IL-6, CCL2/MCP-1, CCL8/MCP-2, CCL7/MCP-3, p27/Kip1, PDGF-AA, SerpinB5/Maspin, Snail, SPARC and VEGF all significantly increased compared to the normal samples. As reported, eNOS, endostatin, HIF-1 α , IL-6, CCL2/MCP-1, CCL8/MCP-2, CCL7/MCP-3, Tie and VEGF involve in the metastasis of tumor. Metastasis is the main cause leading to death in all types of cancer containing GC, OS and ES.

3.2. Higher cytokines levels in GC, OS and ES clinical samples

Four cytokines including MCP1, MCP2, MCP3 and IL-6 in GC, OS and ES tissues were determined

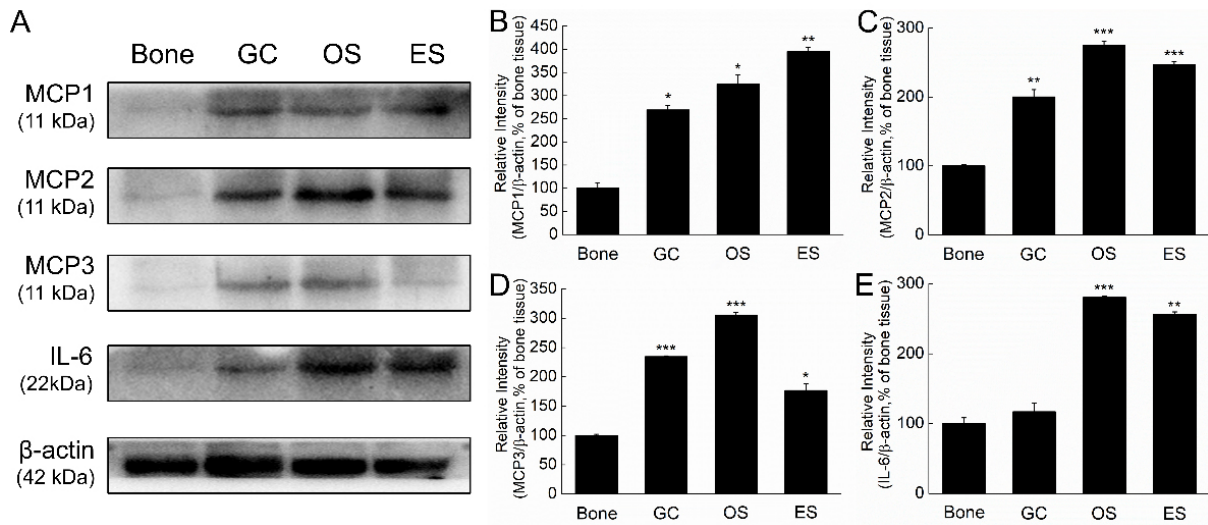


Fig. 2. Higher levels of tumor-associated cytokines in GC, OS or ES clinical samples. A. MCP1, MCP2, MCP3 and IL-6 were determined by Western blot. MCP1 (B), MCP2 (C) and MCP3 (D) levels in GC, OS and ES are significantly higher than the bone samples, and IL-6 significantly increased in OS and ES (E). The data are shown as the means \pm SD, * $P < 0.05$, ** $P < 0.01$ and *** $P < 0.001$ versus the normal bone samples.

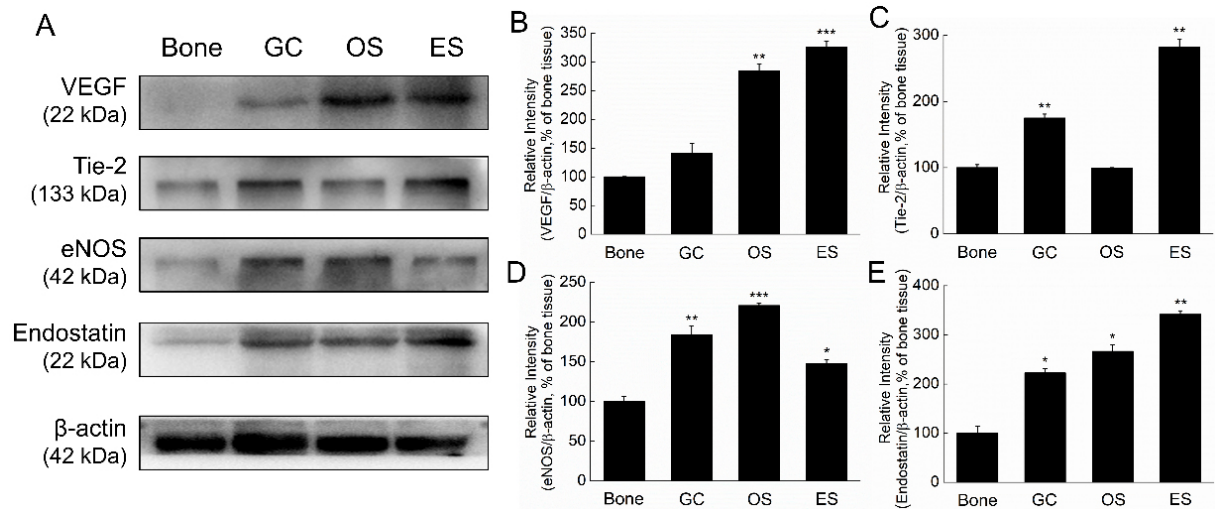


Fig. 3. Expression levels of angiogenesis and anti-angiogenesis protein in GC, OS and ES clinical tissues. A. VEGF, Tie-2, eNOS, endostatin and HIF-1 α were determined by Western blot analysis. B–F. Quantification of VEGF, Tie-2, eNOS, endostatin and HIF-1 α protein expression was performed by densitometric analysis and β -actin was acted as an internal control. The data are shown as the means \pm SD, * $P < 0.05$, ** $P < 0.01$ and *** $P < 0.001$ versus the normal bone samples.

by western blot. Our results showed that MCP1, MCP2 and MCP3 levels were all significantly higher than the normal bone tissues (Fig. 2A). The data was consistent to the proteome profiling analysis. ES tissue expressed higher MCP1 than GC and OS, and OS expressed higher MCP2 and MCP3 than GC and ES. Different from the proteome profiling analysis, IL-6 levels only significantly increased in OS and ES samples, but not in GC (Fig. 2A). Expression of MCP1 level in ES was higher than GC and OS (Fig. 2B),

and OS tissues expressed higher levels of MCP2, MCP3 and IL-6 (Fig. 2C and D). Comparing to OS and ES samples, GC expressed lowest MCP1, MCP2 and IL-6 (Fig. 2B, C and E).

3.3. Expression of angiogenesis and anti-angiogenesis factors in GC, OS and ES clinical samples

To compare the metastasis ability between the three bone tumors, expression levels of pro-angiogenic and anti-angiogenic factors were further determined by Western blot (Figs 2A and 3A).

Among the three bone tumors, ES and OS tissues expressed significantly higher levels of VEGF than the normal samples, but no significant difference was observed between GC and the control (Fig. 3B). For Tie-2, higher levels in GC and ES tissue were observed, but no significant difference was shown between OS and normal tissues (Fig. 3C). Additionally, both eNOS and endostatin levels in the three bone tumor samples were significantly higher than the normal tissues (Fig. 3D and E). However, no significant difference was determined between the three bone tumors and the normal tissues (Fig. 3F).

Based on the data, the pro-angiogenic factors containing VEGF, eNOS and Tie-2 increased in the bone tumor samples with the increase of anti-angiogenic factors endostatin. In GC sample, Tie-2, eNOS and endostatin levels were higher than the control, but not VEGF (Fig. 3B–E). In OS tissues, the expression levels of VEGF, eNOS and endostatin significantly increased, but not Tie-2 (Fig. 3B–E). In ES sample, the factors including VEGF, Tie-2, eNOS and endostatin were all significantly enhanced (Fig. 3B–E).

4. Discussion and conclusion

Invasive tumor metastasis is based on angiogenesis which constitutes an important factor in cancer progression [11]. VEGF is a master regulator of angiogenesis which has many functions including stimulation of vasculogenesis, inflammation, and vascular permeability [12]. HIF-1 α -p300/CREB binding protein complex regulated the encoding VEGF by binding to a HIF-responsive element [13]. Similar to our results, the expression of VEGF are strong in 58.3% of 86 clinical osteosarcoma samples by immunohistochemical staining [14]. Moreover, the high expression of VEGF was determined in GC patients' samples using immunohistochemistry, and the expression of VEGF have been linked the biological aggressiveness of GC [15]. However, our results showed no significant difference of HIF-1 α expression among four types of tissues, which suggested that other factors might contribute to the high expression of VEGF.

Other significantly increased molecules responsible for angiogenesis containing eNOS, endostatin and Tie-2 have been found in the bone tumor samples. Nitric oxide (NO) that is predominantly synthesized by eNOS in vascular endothelial cells promotes angiogenesis directly and functions both upstream and downstream of angiogenic stimuli [16]. On the contrary, endostatin is one of the most widely studied endogenous angiogenesis inhibitors [17]. Though recombinant human endostatin have been used as a drug treating non-small cell lung cancer, why tumors produce more endostatin and how tumor-derived endostatin act on tumor progression is still vague. Tie-2 also plays an important role in vascular development and maintenance and interacts with angiopoietins [18]. Overall, angiogenesis is tightly controlled by pro-angiogenic and anti-angiogenic regulators to maintain the dynamic homeostasis [19].

Tumor-associated inflammatory cytokines are closely associated with the progression of bone tumor, several cytokines were selected and further analyzed in GC, OS and ES clinical samples. Monocyte chemoattractant proteins (MCPs), all belong to CC chemokines, were initially identified as regulators of leukocyte trafficking, they play critical roles in numerous pathological process such as cancer progression [20]. MCP1, a member of MCPs also known as chemokine ligand 2 (CCL2), is an important

proinflammatory cytokine involving a variety of inflammatory response and promoting tumor proliferation, invasion and metastasis. Blockage of MCP1 could attenuate the progression of multiply of cancers [21]. The invasion activity of prostate cancer cells co-cultured with monocyte-lineage cells increased by the MCP1 [22]. It has been reported that osteolysis mediated by OS could be inhibited by attenuation of tumor expression of MCP-1 and RANKL *in vivo* mouse model [23]. Similar to our results, it has been reported that MCP-1 are significantly increased in GC patients' serum [24]. MCP2 induced the migration and invasion of tumor cells *in vitro* through NF- κ B signaling in esophageal squamous cell carcinoma [25]. However, few studies were reported on the effect of MCP-2 on GS, OS and ES. MCP3, derived from tumor cells, play a significant role in cancer invasion and metastasis by down-regulation of tumor suppressor Let-7d [26]. In colon cancer, MCP3 caused an enhancement of cell migration and invasion through ERK/JNK activation [27]. IL-6 is widely studied in cancer progression, and its classical anti-inflammatory pathway is promoted by signal transducer and activator of transcription 3 (STAT3) [28]. In lung adenocarcinoma, IL-6 and VEGF was positively correlated to tumor microvasculature density [29]. Many studies have reported that bone tumors have high level of IL-6 expression, which suggested IL-6 plays an important role in the progression of the bone tumors. IL-6 induced EMT of OS via the STAT3/Snail pathway [30], and increased IL-6 regulated NF- κ B signals can increase the mobility of OS. Combined to our data, IL-6 may be a potential target for the bone tumor.

Acknowledgments

The study is supported by The National Natural Science Foundation of China (grant no. 81702849) and Jilin Province Science and Technology Department of Natural Science Project (no. 20200201605JC).

Authors' contributions

Guirong Zhang designed the study, BoDou, Tianrui Chen and Qiubo Chu performed the experiments and analyzed data, and Zhaoli Meng wrote and edited the manuscript. All authors read and approved the final manuscript.

Ethics approval and consent to participate

The research protocol was approved by the Ethics Committee of the Second Military Medical University, and written informed consent was obtained from all participants. All methods were performed in accordance with the relevant guidelines.

Conflict of interest

The authors confirm that they have no competing interest.

References

- [1] Palmerini E, Picci P, Reichardt P, Downey G. Malignancy in giant cell tumor of bone: a review of the literature. *Technol Cancer Res Treat.* 2019; 18: 1533033819840000. doi: 10.1177/1533033819840000.

- [2] Wu C, Wang Q, Li Y. Prediction and evaluation of neoadjuvant chemotherapy using the dual mechanisms of (99m)Tc-MIBI scintigraphy in patients with osteosarcoma. *J Bone Oncol*. 2019; 17: 100250. doi: 10.1016/j.jbo.2019.100250.
- [3] Gupta R, Seethalakshmi V, Jambhekar NA, Prabhudesai S, Merchant N, Puri A, et al. Clinicopathologic profile of 470 giant cell tumors of bone from a cancer hospital in western India. *Ann Diagn Pathol*. 2008; 12(4): 239–48. doi: 10.1016/j.anndiagpath.2007.09.002.
- [4] Lau YS, Sabokbar A, Gibbons CL, Giele H, Athanasou N. Phenotypic and molecular studies of giant-cell tumors of bone and soft tissue. *Hum Pathol*. 2005; 36(9): 945–54. doi: 10.1016/j.humpath.2005.07.005.
- [5] Kumta SM, Huang L, Cheng YY, Chow LTC, Lee KM, Zheng MH. Expression of VEGF and MMP-9 in giant cell tumor of bone and other osteolytic lesions. *Life Sci*. 2003; 73(11): 1427–36. doi: 10.1016/s0024-3205(03)00434-x.
- [6] Karkare S, Allen KJH, Jiao R, Malo ME, Dawicki W, Helal M, et al. Detection and targeting insulin growth factor receptor type 2 (IGF2R) in osteosarcoma PDX in mouse models and in canine osteosarcoma tumors. *Sci Rep*. 2019; 9(1): 11476. doi: 10.1038/s41598-019-47808-y.
- [7] Salvatore V, Focaroli S, Teti G, Mazzotti A, Falconi M. Changes in the gene expression of co-cultured human fibroblast cells and osteosarcoma cells: the role of microenvironment. *Oncotarget*. 2015; 6(30): 28988–98. doi: 10.18632/oncotarget.4902.
- [8] Zhou S. TGF-beta regulates beta-catenin signaling and osteoblast differentiation in human mesenchymal stem cells. *J Cell Biochem*. 2011; 112(6): 1651–60. doi: 10.1002/jcb.23079.
- [9] Iwamoto Y. Diagnosis and treatment of Ewing's sarcoma. *Jpn J Clin Oncol*. 2007; 37(2): 79–89. doi: 10.1093/jjco/hyl142.
- [10] Zhu L, McManus MM, Hughes DP. Understanding the biology of bone sarcoma from early initiating events through late events in metastasis and disease progression. *Front Oncol*. 2013; 3: 230. doi: 10.3389/fonc.2013.00230.
- [11] Xie L, Ji T, Guo W. Anti-angiogenesis target therapy for advanced osteosarcoma (Review). *Oncol Rep*. 2017; 38(2): 625–36. doi: 10.3892/or.2017.5735.
- [12] Mazure NM, Chen EY, Yeh P, Laderoute KR, Giaccia AJ. Oncogenic transformation and hypoxia synergistically act to modulate vascular endothelial growth factor expression. *Cancer Res*. 1996; 56(15): 3436–40.
- [13] Kong D, Park EJ, Stephen AG, Calvani M, Cardellina JH, Monks A, et al. Echinomycin, a small-molecule inhibitor of hypoxia-inducible factor-1 DNA-binding activity. *Cancer Res*. 2005; 65(19): 9047–55. doi: 10.1158/0008-5472.
- [14] Liu Y, Zhang F, Zhang Z, Wang D, Cui B, Zeng F, et al. High expression levels of Cyr61 and VEGF are associated with poor prognosis in osteosarcoma. *Pathol Res Pract*. 2017; 213(8): 895–9. doi: 10.1016/j.prp.2017.06.004.
- [15] Wu Z, Yin H, Liu T, Yan W, Li Z, Chen J, et al. MiR-126-5p regulates osteoclast differentiation and bone resorption in giant cell tumor through inhibition of MMP-13. *Biochem Biophys Res Commun*. 2014; 443(3): 944–9. doi: 10.1016/j.bbrc.2013.12.075.
- [16] Fukumura D, Kashiwagi S, Jain RK. The role of nitric oxide in tumour progression. *Nat Rev Cancer*. 2006; 6(7): 521–34. doi: 10.1038/nrc1910.
- [17] O'Reilly MS, Boehm T, Shing Y, Fukai N, Vasios G, Lane WS, et al. Endostatin: an endogenous inhibitor of angiogenesis and tumor growth. *Cell*. 1997; 88(2): 277–85. doi: 10.1016/s0092-8674(00)81848-6.
- [18] Hansen TM, Singh H, Tahir TA, Brindle NP. Effects of angiopoietins-1 and -2 on the receptor tyrosine kinase Tie2 are differentially regulated at the endothelial cell surface. *Cell Signal*. 2010; 22(3): 527–32. doi: 10.1016/j.cellsig.2009.11.007.
- [19] Ribatti D, Nico B, Crivellato E, Roccaro AM, Vacca A. The history of the angiogenic switch concept. *Leukemia*. 2007; 21(1): 44–52. doi: 10.1038/sj.leu.2404402.
- [20] Chen Q, Sun W, Liao Y, Zeng H, Shan L, Yin F, et al. Monocyte chemotactic protein-1 promotes the proliferation and invasion of osteosarcoma cells and upregulates the expression of AKT. *Mol Med Rep*. 2015; 12(1): 219–25. doi: 10.3892/mmr.2015.3375.
- [21] An J, Xue Y, Long M, Zhang G, Zhang J, Su H. Targeting CCR2 with its antagonist suppresses viability, motility and invasion by downregulating MMP-9 expression in non-small cell lung cancer cells. *Oncotarget*. 2017; 8(24): 39230–40. doi: 10.18632/oncotarget.16837.
- [22] Lindholm PF, Sivapurapu N, Jovanovic B, Kajdacsy-Balla A. Monocyte-induced prostate cancer cell invasion is mediated by chemokine ligand 2 and nuclear factor-kappaB activity. *J Clin Immunol*. 2015; 6(2). doi: 10.4172/2155-9899.1000308.
- [23] Ohba T, Cole HA, Cates JM, Slosky DA, Haro H, Ando T, et al. Bisphosphonates inhibit osteosarcoma-mediated osteolysis via attenuation of tumor expression of MCP-1 and RANKL. *J Bone Miner Res*. 2014; 29(6): 1431–45. doi: 10.1002/jbmr.2182.
- [24] Xu L, Luo J, Jin R, Yue Z, Sun P, Yang Z, et al. Bortezomib inhibits giant cell tumor of bone through induction of cell apoptosis and inhibition of osteoclast recruitment, giant cell formation, and bone resorption. *Mol Cancer Ther*. 2016; 15(5): 854–65. doi: 10.1158/1535-7163.
- [25] Zhou J, Zheng S, Liu T, Liu Q, Chen Y, Tan D, et al. MCP2 activates NF-kappaB signaling pathway promoting the migration and invasion of ESCC cells. *Cell Biol Int*. 2018; 42(3): 365–72. doi: 10.1002/cbin.10909.
- [26] Murray Peter J, Allen Judith E, Biswas Subhra K, Fisher Edward A, Gilroy Derek W, Goerdts S, et al. Macrophage activation and polarization: nomenclature and experimental guidelines. *Immunity*. 2014; 41(1): 14–20. doi: 10.1016/j.immuni.2014.06.008.

- [27] Lee YS, Kim SY, Song SJ, Hong HK, Lee Y, Oh BY, et al. Crosstalk between CCL7 and CCR3 promotes metastasis of colon cancer cells via ERK-JNK signaling pathways. *Oncotarget*. 2016; 7(24): 36842–53. doi: 10.18632/oncotarget.9209.
- [28] Rose-John S. Interleukin-6 family cytokines. *Csh Perspect Biol*. 2018; 10(2). doi: 10.1101/cshperspect.a028415.
- [29] Huang Q, Duan L, Qian X, Fan J, Lv Z, Zhang X, et al. IL-17 promotes angiogenic factors IL-6, IL-8, and vegf production via stat1 in lung adenocarcinoma. *Sci Rep*. 2016; 6: 36551. doi: 10.1038/srep36551.
- [30] Kong G, Jiang Y, Sun X, Cao Z, Zhang G, Zhao Z, et al. Irisin reverses the IL-6 induced epithelial-mesenchymal transition in osteosarcoma cell migration and invasion through the STAT3/Snail signaling pathway. *Oncol Rep*. 2017; 38(5): 2647–56. doi: 10.3892/or.2017.5973.